SHIP MANEUVERING PREDICTION
USING GREY BOX FRAMEWORK VIA ADAPTIVE RM-SVM
WITH MINOR RUDDER

Bin Mei [a]
Licheng Sun [a]
Guoyou Shi [a]
Xiaodong Liu [b]
[a] Dalian Maritime University, The People's Republic of China
[b] Dalian University of Technology, The People's Republic of China

ABSTRACT

A grey box framework is applied to model ship maneuvering by using a reference model (RM) and a support vector machine (SVM) (RM-SVM). First, the nonlinear characteristics of the target ship are determined using the RM and the similarity rule. Then, the linear SVM adaptively fits the errors between acceleration variables of RM and target ship. Finally, the accelerations of the target ship are predicted using RM and linear SVM. The parameters of the RM are known and conveniently acquired, thus avoiding the modeling process. The SVM has the advantages of fast training, quick simulation, and no overfitting. Testing and validation are conducted using the ship model test data. The test case reveals the practicability of the RF-SVM based modeling method, while the validation cases confirm the generalization ability of the grey box framework.

INTRODUCTION

A report by the International Maritime Organization (IMO) pertaining to the global use of autonomous systems indicated that autonomous ships may be launched soon [1]. Ship maneuvering modeling is the key element of ship motion prediction (kinematics and kinetics), simulation and control of autonomous ship navigation, and collision avoidance [2]. Ship maneuverability has received increasing attention from the shipping industry.

Generally, there are several primary methods based on captive model test, free model test, full-scale trials, and computational fluid dynamics (CFD) [2-4] which are used for maneuvering simulations. The reports of the International Towing Tank Conference (ITTC) offer a broad overview of many available ship modeling methods [4]. To obtain the ship hydrodynamic force and ascertain the hydrodynamic coefficients, captive model tests, such as planar motion mechanism (PMM) and circular motion test (CRM), and other complicated and expensive tests, must be used repeatedly [5]. CFD is a crucial method for theoretical calculations and has a long history. As the performance of computers has been improving with time, CFD can be utilized much more effectively. However, CFD analyses need human experience to build a suitable grid, and remain excessively time-consuming for online ship motion prediction [3]. The overview of methods to develop a ship maneuvering model reveals that system identification has a significantly lower

cost and requires considerably lower effort. However, this method is not as precise as the free running model test, the captive model test, or CFD [4]. This implies that, despite their drawbacks, the captive model tests and CFD realize a more accurate model. Therefore, to increase its accuracy, the system identification method should be improved on the basis of free model tests and full-scale sea trials.

The system identification method fits the test data and conducts generalization ability simultaneously. When a ship is sailing on the sea, its sailing conditions change constantly due to the action of environmental disturbances and changing load conditions. For ship motion control and prediction, the system identification method can simulate the future trajectory and velocity by using sensors. Researchers of ship motion identification modeling have made many attempts to deal with this problem [6-13], and their results are classified as white box, black box, and grey box identification.

For white box system identification, Abkowitz introduced an EKF to identify model parameters during ship sea trials [6]. Other researchers used partial least squares regression, multi-innovation least squares (MILS), and linear support vector machine (LS-SVM) approaches to verify the parameters [7-9]. However, the parameters could not be identified using partial least squares regression for a ship in motion under wind or wave disturbances, and MILS and LSVM did not yield accurate simulations. Kallstrom used the pseudo random binary sequence (PRBS) as the maneuver signal [10]. Yoon applied ridge regression to figure out the parameters, and improved the PRBS and D-optimal maneuver scheme [11]. Sutulo and Soares presented an offline system modeling method using five different learning metrics and genetic algorithm (GA) based parameter optimization [12]. However, the GA only obtains the learning parameters with a fixed interval on the basis of theoretical or database methods.

Many studies have been conducted on black box system identification. Haddara obtained an optimal effect by estimating derivatives with neural networks, but the network training was time consuming [13]. Wang (2015) proposed a fuzzy neural network for system identification modeling [14]. Faller presented a maneuvering motion model by using a recursive neural network (RNN), for which a number of numerous turning circle and zigzag maneuvers were utilized as training tests [15]. Moreira proposed an RNN maneuvering simulation model for turning circle and zigzag maneuvers, but this method also required a lot of training tests [16]. Oskin presented an RNN to identify a ship motion response model that neglects ship speed prediction [17]. On the basis of multiple tests, Bai used the locally weighted learning to predict maneuvering motion by using the black box structure. However, the maneuver scheme for identification was not suitable as good seamanship handling required [18]. Zhu used a least squared SVM and optimized it with the artificial bee colony method, but the surge velocity was not verified for a zigzag test [19]. Luo proposed a method in which the reconstruction of sample data was identified using an SVM, and no verification was conducted for the turning test [20]. Thus, system identification methods require considerable ship

motion test data and have poor generalization ability. For the grey box identification, Wang used SVM to get the ship maneuvering model without ship's principal particulars [26].

Motivated by these observations, we aim to address the problems in ship motion identification. Despite improvements in the precision of system identification for ship motion since the ITTC 2005, some difficulties have not been overcome yet.

Firstly, it is not very feasible to use simulation data for system identification. When the simulation test data is without noise, it has higher quality and can be easily used for identification. However, in practical scenarios, the test data contains measurement errors and disturbances from the sea environment. Secondly, the period, frequency and other characteristics of the input signals in the simulation test, such as the sinusoidal rudder angle and pulse signals [14], and the PRBS and D-optimal signals [10,11], are relatively broad. However, a sinusoidal rudder angle cannot be easily obtained for the steering control system. Moreover, for sea trials, the IMO proposed a maximum allowable rudder angle (+20°/–20°) as a test scheme standard for ship maneuverability. Therefore, although the identification of simulation data is better than trial data, it is difficult to obtain training data in full-scale trials.

The sea trials are only conducted in light ballast or heavy ballast conditions. Therefore, for using the data of the ship trial test as the identification data, the ship maneuvering ability should be converted from the ballast condition to the full load condition [21]. Thus, the sea trial test is not convenient for identification modeling. This implies that the test data under the full load condition are more suitable for ship operation with inadequate excitation. The aim of this study is to improve the precision of identification modeling and to reduce the data set for identification, thus reducing the effort, time, and cost required for modeling. These problems are addressed using the features of the reference model (RM).

PROBLEMS AND PRELIMINARIES

The aim of the grey box approach is to model ship maneuvering and describe the trajectory and velocity of the ship during navigation on the sea. In this section, the problems of ship maneuvering are presented and simplified. Then, the grey box structure is correlated with ship velocities and accelerations, and utilized to address the aforementioned problems.

PROBLEMS

During sea navigation, the ship motion is typically described in three degrees of freedom (3 DOF). A 3-DOF model is equivalent to a horizontal plane model with surge, sway, and yaw motion. There are two assumptions for this model. Assumption A: On the basis of the rigid-wall boundary condition, the free surface is regarded as a fixed horizontal plane [22]. Assumption B: The 3-DOF model is a specific horizontal plane model. The motions can be decoupled into

longitudinal and lateral motions. Moreover, sway and yaw are coupled. On the basis of these assumptions, the model can be described as Equation (1) [23]:

$$\begin{cases} m - X_{\dot{u}}\dot{u} = f_1(u,v,r,\delta) \\ (m - Y_{\dot{v}})\dot{v} + (mx_G - Y_{\dot{r}})\dot{r} = f_2(u,v,r,\delta) \\ (mx_G - N_{\dot{v}})\dot{v} + (I_z - N_{\dot{r}})\dot{r} = f_3(u,v,r,\delta) \end{cases} \qquad \textbf{(1)}$$

where m represents the mass of the ship; x_G represents the gravity center of ship's mass; (x,y) is the trajectory of the ship's gravity center; ψ is the ship course; u,v,r are the velocities of surge, sway, and yaw motion, respectively; I_z is the moment of inertia; and $X_{\dot{u}}, Y_{\dot{v}}, Y_{\dot{r}}, N_{\dot{v}}$ and $N_{\dot{r}}$ are constants. Equation (1) can be rewritten as Equation (2):

$$\begin{cases} \dot{u} = f_1 / (m - X_{\dot{u}}) \\ = G_1(u,v,r,\delta) \\[2mm] \dot{v} = \dfrac{(I_z - N_{\dot{r}}) \cdot f_2 - (mx_G - N_{\dot{v}}) \cdot f_3}{(m - Y_{\dot{v}})(I_z - N_{\dot{r}}) - (mx_G - N_{\dot{v}})(mx_G - Y_{\dot{r}})} \\ = G_2(u,v,r,\delta) \\[2mm] \dot{r} = \dfrac{(m - Y_{\dot{v}}) \cdot f_3 - (mx_G - N_{\dot{v}}) \cdot f_2}{(m - Y_{\dot{v}})(I_z - N_{\dot{r}}) - (mx_G - N_{\dot{v}})(mx_G - Y_{\dot{r}})} \\ = G_3(u,v,r,\delta) \end{cases} \qquad \textbf{(2)}$$

The ship hydrodynamics functions G_1, G_2, and G_3 on the right-hand side of Equation (2) are purely related to the ship maneuver state (u, v, r, δ), which determines ship accelerations.

PRELIMINARIES OF THE GREY BOX FRAMEWORK

To resolve the ship maneuvering problem, system identification modeling is used to quantify the relationship between ship motion velocities and accelerations. RM-SVM is a grey box framework used for system identification. In this section, the concepts of general grey box and RM-SVM are introduced. Then, the framework and flowchart of RM-SVM are presented.

Based on Ljung's description [24], combining the identification model with a nonlinear static model and a linear dynamic model gives a slate grey model. The RM, being a concept from adaptive control [25], is an approximate model of the controlled object. For ship maneuvering, an existing mathematical model can be used as RM, which is a nonlinear static model. Hence, as presented in Figure 2, the nonlinear static model, the RM, and the nonlinear ship motion model are identical and belong to the same category. Then, a linear SVM is used as the learning algorithm, which is equivalent to a linear dynamic model. The dynamic model approximates the error between the target ship and the RM. The conceptual evolution path of the slate grey model, RM,

and ship motion grey box identification model is presented in Figure 1.
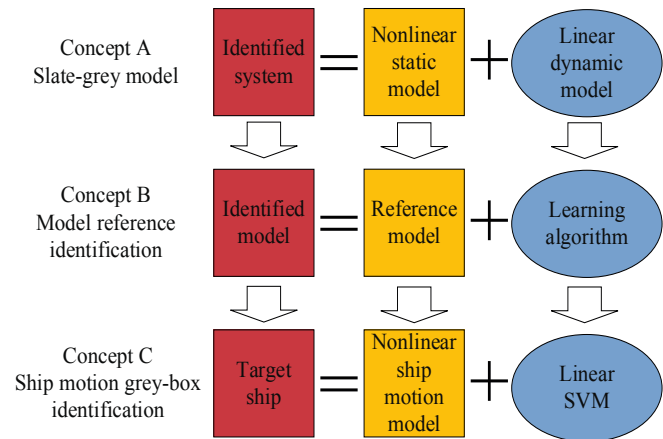

Fig. 1. Conceptual evolution path of the slate grey box, reference model, and ship motion grey box identification frameworks

It is noteworthy that the SVM has been used as grey box [26]. There are three differences between SVM and RM-SVM, although SVM is used in RM-SVM. As shown in Figure 2, firstly, the outputs of SVM and RM-SVM are different. Secondly, the accelerations consist of RM and errors between RM and target ship. Thirdly, the system in SVM is a discrete-time system, while in RM-SVM it is a continuous-time system. Therefore, RM-SVM is different from SVM. Furthermore, SVM is an artificial intelligent (AI) algorithm in RM-SVM, and can be replaced by any other regression algorithm, e.g. neural network, decision trees, and logistic regression. Since the RM can be verified and advanced, RM modeling provides robust estimation of ship velocities when SVM fails.

As presented in Figure 2.b, ship maneuvering is a time-consuming task, and accelerations are selected as inputs and output of the grey box system. The steps of grey box modeling are as follows:

a: Select an existing nonlinear ship maneuvering motion model as the RM.

b: Convert the target ship velocities u_T, v_T, and r_T to the RM velocities u_R, v_R, and r_R, respectively.

c: Calculate the RM accelerations $\dot{u}_R$, $\dot{v}_R$, and $\dot{r}_R$, and the RM velocities u_R, v_R, and r_R; the rudder angle is δ_R.

d: SVM compensates the acceleration errors of the target ship and the RM.

e: Adaptively tune the SVM parameter.

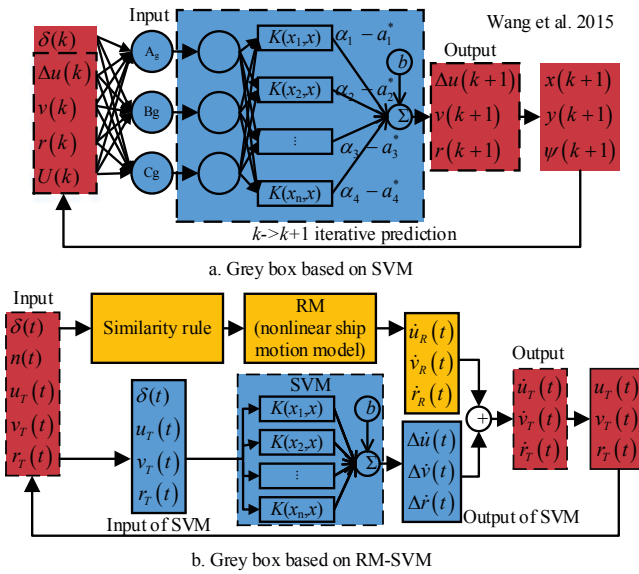a. Grey box based on SVM

b. Grey box based on RM-SVM

Fig. 2. Comparison of grey box framework based on SVM [26] and RM-SVM for ship motion identification modeling

GREY BOX MODELING

In this section, the details and content of the application of the RM-SVM are presented. Firstly, the RM is selected, and then the target ship velocities are converted to the RM. As the third step, the SVM is obtained for use in the RM-SVM. Finally, adaptive tuning of the SVM parameter is done.

SELECTION OF RM

Several models used for ship maneuvering were mentioned in [19]. Nonlinear static models, such as the response model of sway motion, the Mathematical Maneuvering Group (MMG) response model, and the Abkowitz model, can be employed as the RM. It is crucial to select a suitable RM from the existing models. The selected RM should be most suitable for the target ship.

On the basis of [27], we consider the particular vector p as the feature of the ship. Moreover, Cb is the ship block coefficient, Lpp is the length between perpendiculars, B is the ship beam, T is the ship draught, V_0 is the speed of the designed ship, and Ar is the rudder area. Thus, we obtain Equation (3):

$$p = (Cb, \ Lpp / B, \ B / T, \ Lpp / V_0, \ Ar / (Lpp \cdot T)) \quad (3)$$

The matrices P comprise p, which can be expressed as Equation (4):

$$P = (p_1, \ ..., \ p_i, \ ..., \ p_m)^T$$

$$= \begin{pmatrix} Cb_1 & Cb_2 & ... & Cb_n \\ \dfrac{Lpp_1}{B_1} & \dfrac{Lpp_2}{B_2} & ... & \dfrac{Lpp_n}{B_n} \\ \dfrac{B_1}{T_1} & \dfrac{B_2}{T_2} & ... & \dfrac{B_n}{T_n} \\ \dfrac{Lpp_1}{V_{01}} & \dfrac{Lpp_2}{V_{02}} & ... & \dfrac{Lpp_n}{V_{0n}} \\ \dfrac{Ar_1}{Lpp_1 T_1} & \dfrac{Ar_2}{Lpp_2 T_2} & ... & \dfrac{Ar_n}{Lpp_n T_n} \end{pmatrix} \quad (4)$$

Let $\eta_i = (P_{i1}, \ ..., \ P_{ij}, \ ..., \ P_{in})^T$; $m = 5$; $i = 1, 2, ..., m$; and $j = 1, 2, ..., n$. Then, the normalization of the particular matrix P can be given as Equation (5):

$$\zeta_i = \frac{\eta_i}{\|\eta\|_2} = \frac{\eta_i}{(P_{i1}^2 + ... + P_{ij}^2 + ... + P_{in}^2)^{\frac{1}{2}}} \quad (5)$$

Let $Q = (\zeta_1, \ \zeta_2, \ ..., \ \zeta_n)^T$ and $(q_1, \ q_1, \ ..., \ q_n) = Q^T$. The normalization particular vector is q_i. Then, the coefficient γ_i of the relationship between q_1 and q_i can be written as Equation (6):

$$\gamma_i = \frac{COV(q_1, q_i)}{\sigma(q_1)\sigma(q_i)}$$

$$= \frac{E(q_1 q_i) - E(q_1)E(q_i)}{\{E(q_1^2) - E^2(q_1)\}^{\frac{1}{2}}\{E(q_i^2) - E^2(q_i)\}^{\frac{1}{2}}}$$

$$= \frac{\sum q_1 q_i - \dfrac{\sum q_1 \sum q_i}{n}}{\{(\sum q_1^2 - \dfrac{(\sum q_1)^2}{n})(\sum q_1^2 - \dfrac{(\sum q_1)^2}{n})\}^{\frac{1}{2}}} \quad (6)$$

The ship corresponding to the maximum γ is most similar to the target ship and is selected as the RM. In other words, the order and structure of the selected RM are approximately equal to those of the target ship.

CONVERSION OF VELOCITIES

The target ship and the RM have differently designed standard states, therefore the velocities of the target ship should be converted to the RM. Two conversion methods have been proposed by SNAME [28] and Norrbin [29]. In this study, the normalization forms from the study by SNAME [28] were introduced, including ship surge, sway and yaw motion, and rudder angle. These states are expressed as Equation (7):

$$\begin{cases} u_R = u_T(V_{0R} / V_{0T}) \\ v_R = v_T(V_{0R} / V_{0T}) \\ r_R = r_T(V_{0R} / Lpp_R) / (V_{0T} / Lpp_T) \\ \delta_R = \delta_T \end{cases} \quad (7)$$

where $(\cdot)_T$ represents the target ship and $(\cdot)_R$ represents the RM. Here, V_0 is the service speed and Lpp is the length between perpendiculars.

According to Equation (2), the accelerations of the RM are expressed as Equation (8):

$$\begin{cases} \dot{u}_R = G_{1R}(u_R,v_R,r_R,\delta_R) \\ = G_{1R}(u_T\dfrac{V_{0R}}{V_{0T}},v_T\dfrac{V_{0R}}{V_{0T}},r_T\dfrac{V_{0R}}{V_{0T}}\dfrac{Lpp_T}{Lpp_R},\delta_T) \\ \dot{v}_R = G_{2R}(u_R,v_R,r_R,\delta_R) \\ = G_{2R}(u_T\dfrac{V_{0R}}{V_{0T}},v_T\dfrac{V_{0R}}{V_{0T}},r_T\dfrac{V_{0R}}{V_{0T}}\dfrac{Lpp_T}{Lpp_R},\delta_T) \\ \dot{r}_R = G_{3R}(u_R,v_R,r_R,\delta_R) \\ = G_{3R}(u_T\dfrac{V_{0R}}{V_{0T}},v_T\dfrac{V_{0R}}{V_{0T}},r_T\dfrac{V_{0R}}{V_{0T}}\dfrac{Lpp_T}{Lpp_R},\delta_T) \end{cases} \quad (8)$$

SVM

On the basis of the flowchart of ship motion grey box modeling, the function relating the RM and the target ship is modeled through regression learning algorithms, such as SVMs, neural networks, Gauss regression models, and decision trees. In this study, the SVM was utilized [30].

The RM velocities, $x = (u_T, v_T, r_T, \delta_T)$, are defined as the state variables. Then, the acceleration error between the target ship and RM is $y = (G_{1T} - G_{1R}, G_{2T} - G_{2R}, G_{3T} - G_{3R})$. Consider surge acceleration as an example. The Lagrangian function of the linear SVM for the surge acceleration error is defined as Equation (9):

$$L(w_1,b_1,e_1,a_1) = \frac{1}{2}w_1^T w_1 + \frac{1}{2}C_1\sum_{i=1}^{n}e_{1i}^2$$
$$-\sum_{i=1}^{n}a_{1i}\{w_1^T\varphi(x_i)+b_1+e_{1i}-y_{1i}\} \quad (9)$$

By using sequential minimal optimization (SMO) to solve the Lagrangian function, the regression function y_{1i} is obtained as Equation (10):

$$y_{1i} = \sum_{i=1}^{n}a_{1i}K(x,x')+b_1 \quad (10)$$

where C_1 is the regularization factor, e_1 is the regression error, w_1 is the weighted function, b_1 is the bias, and (x,x') is the linear kernel function written as $x\cdot x^T$.

Thus, the surge acceleration of the target ship is $y_{1i} + G_{1R}$. Similarly, the acceleration of the target ship can be expressed by Equation (11):

$$\begin{cases} \dot{u}_T = y_{1i} + G_{1R} = \\ \sum_{i=1}^{n}a_{1i}(u_T,v_T,r_T,\delta_T)\cdot(u_T,v_T,r_T,\delta_T)^T + b_1 \\ +G_{1R}(u_T\dfrac{V_{0R}}{V_{0T}},v_T\dfrac{V_{0R}}{V_{0T}},r_T\dfrac{V_{0R}}{V_{0T}}\dfrac{Lpp_T}{V_{0T}},\delta_T) \\ \dot{v}_R = y_{2i} + G_{2R} = \\ \sum_{i=1}^{n}a_{2i}(u_T,v_T,r_T,\delta_T)\cdot(u_T,v_T,r_T,\delta_T)^T + b_2 \\ +G_{2R}(u_T\dfrac{V_{0R}}{V_{0T}},v_T\dfrac{V_{0R}}{V_{0T}},r_T\dfrac{V_{0R}}{V_{0T}}\dfrac{Lpp_T}{V_{0T}},\delta_T) \\ \dot{r}_R = y_{3i} + G_{3R} = \\ \sum_{i=1}^{n}a_{3i}(u_T,v_T,r_T,\delta_T)\cdot(u_T,v_T,r_T,\delta_T)^T + b_3 \\ +G_{3R}(u_T\dfrac{V_{0R}}{V_{0T}},v_T\dfrac{V_{0R}}{V_{0T}},r_T\dfrac{V_{0R}}{V_{0T}}\dfrac{Lpp_T}{V_{0T}},\delta_T) \end{cases} \quad (11)$$

ADAPTIVE TUNING OF SVM

The insensitive band ε is the SVM parameter that should be tuned. This parameter determines the incorrect sample data to be ignored in the SMO solver. In this study, adaptive tuning based on the pattern search algorithm has been introduced. The search range of ε is $[0,1]$. The parameters ε_1, ε_2, and ε_3 are insensitive bands for surge, sway, and yaw accelerations in Equation (11), respectively. As presented in Figure 3, the following search steps are performed:

Step 1: Prepare the training data for the RM-SVM;
Step 2: Initialize $\varepsilon_1, \varepsilon_2$, and ε_3 in the SVM.
Step 3: Conduct the pattern search.
Step 3.1: Generate the mesh grid of $\varepsilon_1, \varepsilon_2$, and ε_3 ranges
Step 3.2: Conduct SMO on the SVM.
Step 3.3: Simulate the training test.
Step 3.4: Calculate the Pearson correlation coefficient λ between the heading angles obtained from the training test and simulation.
Step 3.5: If the coefficient λ is less than the threshold, then repeat Steps 3.1 to 3.5. Otherwise, go to Step 4.
Step 4: Record the optimal values of ε_1, ε_2, and ε_3.
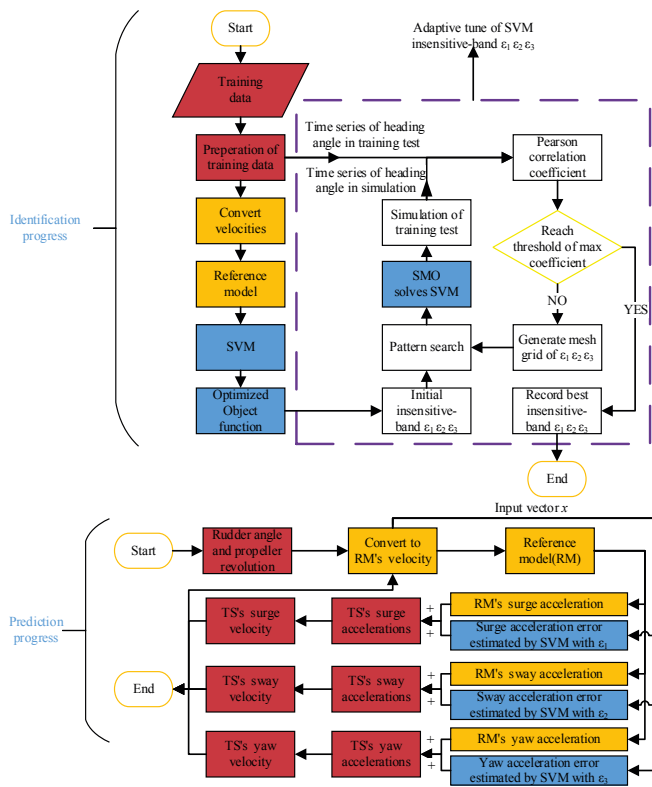
Fig. 3. Adaptive tuning of insensitive bands in SVM and RM-SVM based prediction

PREPARATION

To verify the effectiveness of grey box modeling for ship maneuvering, a free running model test was used and the training test was simulated. Then, the free running model test was validated for estimating the generalization ability.

TEST DATA

KVLCC2 is a benchmark ship used for validation of ship maneuvering models, performed using the system based maneuvering simulation method, CFD-based maneuvering simulation method, and other no simulation methods. Its particulars are presented in Table 1. The data from these two faculties were converted using the prime system [22].

Tab. 1. Particulars of target ship KVLCC2

Particulars	model	Full scale
Scale	45.7	1
Length (m)	7.0	320.0
Maximum breadth (m)	1.17	58.0
Draught (m)	0.46	20.8
Block coefficient	0.81	0.81
Maximum rate of rudder (°)	15.8	2.34
Service speed (knots)	1.18	7.9

The free running model test in basin generates sample points with sampling frequency of 1 Hz. The test type, the rudder angle, and other maneuver scheme information of the test data for study cases are given in Table 2. The tests were performed in the basin, in which the max test rudder of the zigzag maneuver is less than or equal to 20°. Therefore, the test data with minor rudder angle was used to identify the RM-SVM. As presented in Table 3, a relatively small amount of training data was used compared to other studies [15][18][31], and the validation data was different from the training data.

Tab. 2. Training and validation data

Training cases			
Test type	Rudder and heading angle	Sample points	Port/ starboard
Zigzag test	10°/10°	520	starboard
Zigzag test	10°/10°	565	port
Zigzag test	20°/20°	606	starboard
Zigzag test	20°/20°	684	port
Validation cases			
Test type	Rudder angle	Sample points	Port/starboard
Turning circle	35°	1610	starboard
Turning circle	-35°	1151	port

Tab. 3. Comparing test data in the current study and related studies

Training data		Current study	Bai [18]	Wang [31]	Hess [15]
Zigzag	Contained	Yes	Yes	Yes	Yes
	NO. of Case	4	4	2	2
	Max rudder	20	30	20	20
Turning circle	Contained	No	Yes *	Yes	Yes
	NO. of Case	No	4*	2	4
	Max rudder	No	30	15	35
Validation test different from training		Yes	No	No	No

The 20°/20° zigzag test is presented as an example in Figure 4. Spline filters were used to indicate sway velocity and sway acceleration.
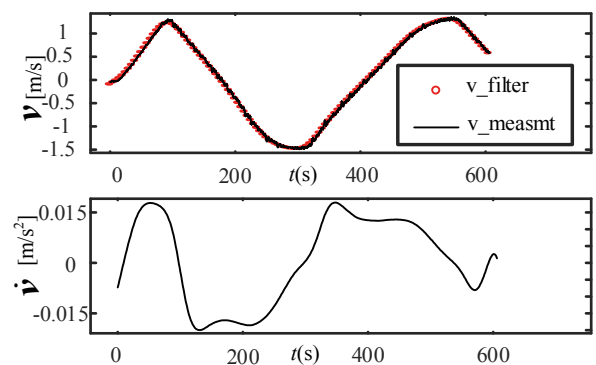

Fig. 4 Sway velocity and acceleration obtained from the filter

RM FOR KVLCC2

Four RMs were used for selecting a proper RM for KVLCC2 [21][23]. The particulars are presented in Table 4. On the basis of the selection conducted to obtain suitable progress in grey box modeling, the correlation coefficients γ between the RMs and KVLCC2 were estimated (-0.5758, 0.8510, -0.8873, and -0.7228). The maximum γ was 0.8510. Therefore, the "Tanker" was selected as the RM.

Tab. 4. Particulars of the Tanker RM

Name	KVLCC2	Mariner [23]	Tanker [23]	SR108 [21]	PCC [21]
Structure	***	Abkowitz	Abkowitz	MMG	MMG
Cb	0.90	0.60	0.83	0.56	0.55
Lpp/B	5.52	6.95	6.39	6.89	5.60
B/T	2.79	3.10	2.58	2.99	3.93
Lpp/V_0	40.1	20.9	37.0	14.1	≈ 18.0
$Ar/(LppT)$	1/48.7	1/83.1	$\approx 1/61.0$	1/45.8	1/39.8

ERRORS BETWEEN RM AND KVLCC2

Following Equation (7), the velocities of KVLCC2 were converted to those of the RM Tanker. Moreover, u_R, v_R, r_R, and δ_R were selected as the inputs for Tanker, and the outputs were $\dot{u}_R$, $\dot{v}_R$, and $\dot{r}_R$. Figure 5 compares the accelerations $\dot{u}_R$, $\dot{v}_R$, and $\dot{r}_R$ with $\dot{u}_T$, $\dot{v}_T$, and $\dot{r}_T$. The result of the comparison is approximated by a line. The relationship coefficients are 0.99, 0.94, and 0.87, which implies that the nonlinear dynamics of KVLCC2 is very well replicated by the Tanker.
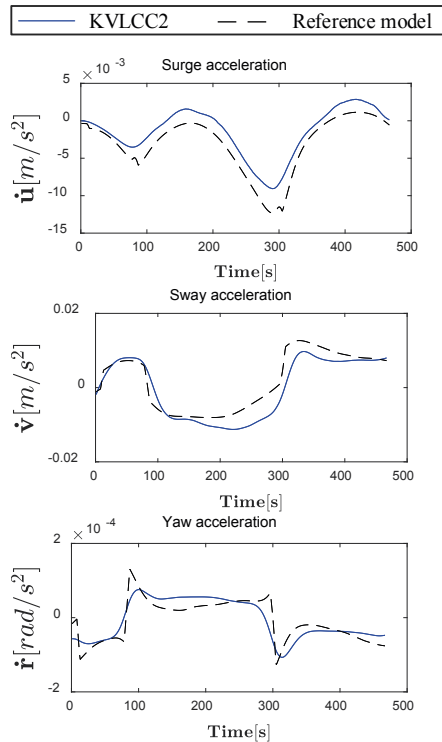

Fig. 5. Comparing accelerations of KVLCC2 and RM

CASE STUDIES

In order to illustrate the prediction performance of the presented grey box model based on RF-SVM, four zigzag tests: 10°/10°, -10°/-10°, 20°/20°, and -20°/-20° were used for training. After that, two validation cases of 35° and -35° turning circle were tested.

ADAPTIVE TUNING OF INSENSITIVE BAND

The parameters ε_1, ε_2, and ε_3 are the insensitive bands for surge, sway, and yaw accelerations. On the basis of adaptive tuning steps, a 20°/20° zigzag test was chosen as the simulation test. The Pearson correlation coefficient λ of the heading angle in the 20°/20° zigzag test was calculated. The optimal insensitive bands obtained from the pattern search correspond to the maximum value of coefficient λ_{max}. As presented in Figure 6, ε_1, ε_2, ε_3, and λ change with the iteration of the pattern search and converge to 0.005, 1, 1, and 0.993, respectively.
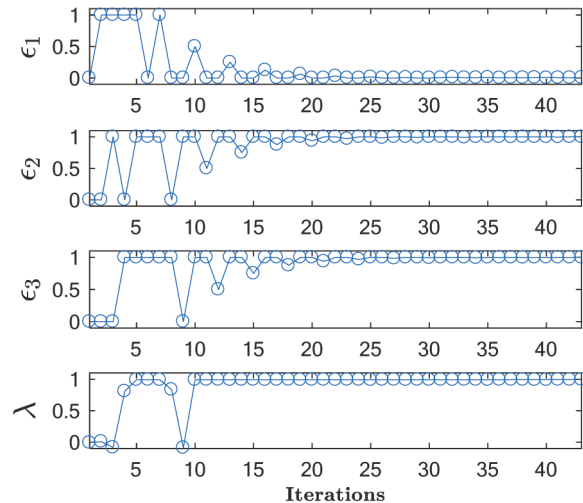

Fig. 6 Iterations of ε_1, ε_2, ε_3, and λ

TRAINING CASE FOR 20°/20° ZIGZAG MANEUVER

To assess the effectiveness of the RM-SVM approach, a training case was simulated. By using Equation (10), the 20°/20° zigzag maneuver was predicted and the heading, velocities, and trajectory were acquired. Then, the results were compared with those of the CFD method from Hyundai Maritime Research Institute (HMRI) presented by Sung [32] and model experiments from NMRI presented by Yasukawa [33]. The results of the above three methods were further compared with those from the free running model test called EXP-MARIN and performed at the Maritime Research Institute Netherlands (MARIN). However, the studies [32] and [33] have included headings rather than velocities. The variables presented in Figure 7 were made dimensionless using the method proposed by Norrbin [29].

Figure 7 shows that RM modeling has the advantages of robust prediction and base estimation. Especially, the base estimation of ship velocities by RM is labeled, and more accurate estimation of RM-SVM is shown.

The first and second overshoot angles (OSA) are presented in Table 5. Their comparison reveals that the RM-SVM has optimal performance and prediction accuracy for the training data. The prediction of the training test is not very accurate. When the overfitting occurs, the training data fits effectively, but lower accuracy is attained for the validation data. The accuracy of the prediction for the training test of the 20°/20° zigzag maneuver is acceptable, which implies that the validation test has an optimal generalization ability.

Tab. 5. OSA predictions of 20°/20 zigzag maneuver obtained from various methods

Methods	EXP-MARIN	EFD-NMRI	RM-SVM	CFD-HMRI
1st OSA	13.8	10.9	11.8	11.7
2nd OSA	14.9	17.0	14.3	16.5

the presented method using the RM-SVM. On the basis of Equation (11), the 35° turning circle case was used for RM-SVM performance validation. After that, the results of the CFD-PMM simulation from the Shanghai Jiao tong University (CFD-SJT) [34], the experimental fluid dynamics (EFD) method from NMRI (proposed by Hironori Yasukawa) [33], and the CFD of HMRI developed by Sung and Park [32] were collected. The results of these methods and the proposed method were compared with the EXP-MARIN free running model test, which is considered most accurate. The surge, sway, and yaw speeds are included in CFD-SJT merely. Thus, the velocities obtained using the proposed method were compared with those obtained using CFD-SJT. Moreover, the trajectory obtained using the proposed method was compared with those from EFD-NMRI, CFD-HMRI, and CFD-SJT.

The time-histories of variables predicted by the aforementioned methods for 35° turning circle test are given in Figure 8.
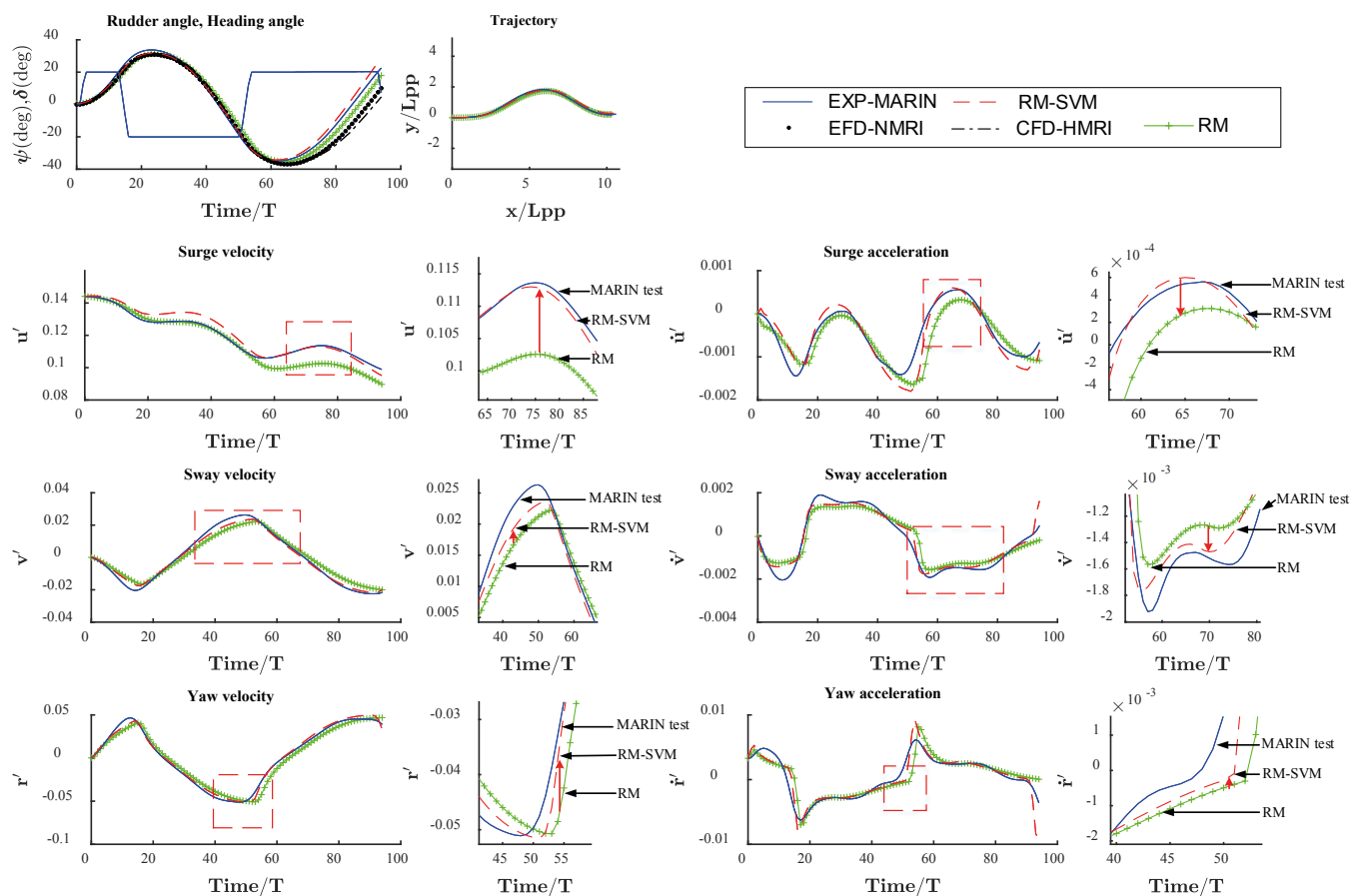

Fig. 7. Prediction variables of 20°/20° zigzag test

VALIDATION CASE FOR GENERALIZATION ABILITY OF 35° TURNING CIRCLE

Being an AI algorithm, SVM should be verified. The same refers to the RM-SVM grey box. Therefore, a validation case was simulated to show the generalization ability of
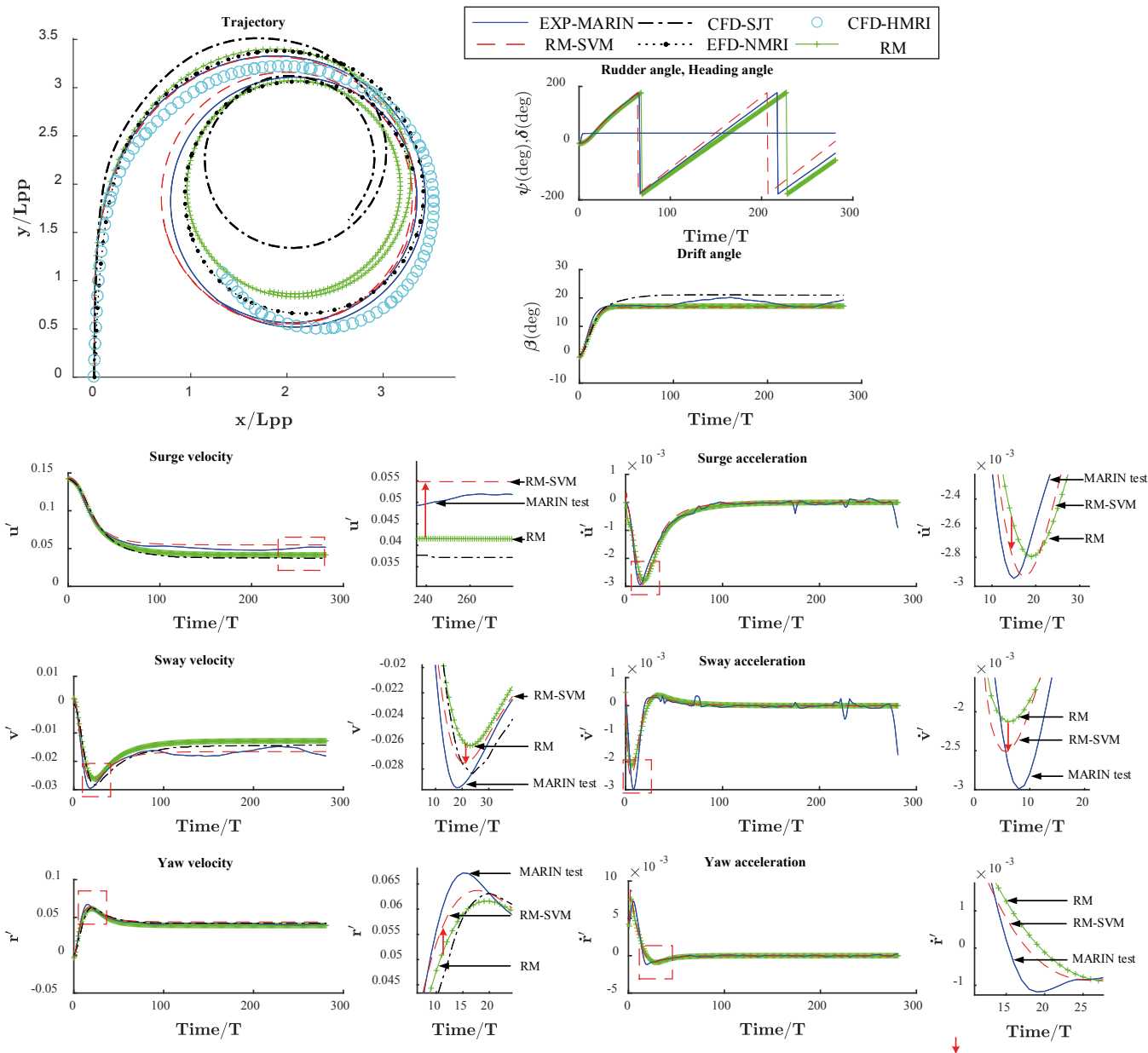
Fig. 8. Prediction variables of 35° turning circle for generalization ability validation

The geometries of the turning circles obtained using different methods are compared in Table 6. The precision of the advance predicted by RM-SVM is outstanding, while the predicted tactical diameter obtained from RM-SVM is average.

Tab. 6. Advances and tactical diameters predicted by different methods for the 35° turning circle case

Methods	EXP-MARIN	EFD-NMRI	RM-SVM	CFD-HMRI	CFD-SJT
$A_D^{'}$	3.25	3.31	3.22	3.12	3.63
$D_T^{'}$	3.34	3.36	3.20	3.4	2.87

VALIDATION CASE FOR GENERALIZATION ABILITY OF −35° TURNING CIRCLE

The -35° turning circle is another validation case for verifying generalization ability of the proposed method. As presented in Figure 9 and Table 7, the variables in the method proposed by Norrbin are dimensionless. The advance predicted by the RM-SVM is similar to the best of those predicted by other methods, while the tactical diameter is average. The approximation ability of RM is shown in Figure 9.
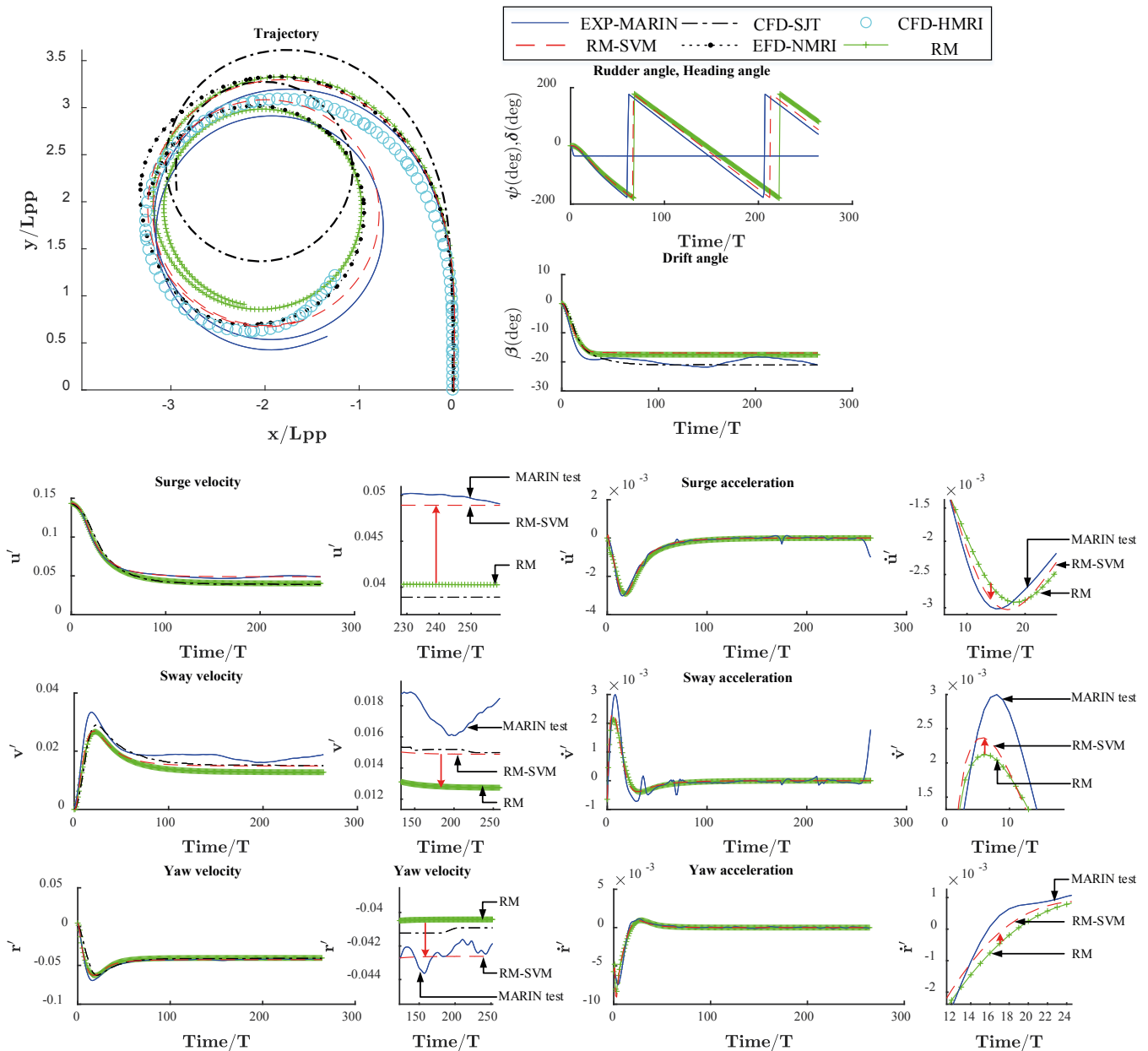
Fig. 9. Prediction variables of −35° turning circle for generalization ability validation

Tab. 7. Advances and tactical diameters predicted by different methods for the -35° turning circle case

Methods	EXP-MARIN	EFD-NMRI	RM-SVM	CFD-HMRI	CFD-SJT
$A_D^{'}$	3.25	3.26	3.26	3.00	3.75
$D_T^{'}$	3.34	3.26	3.24	3.14	2.88

ANALYSIS

The kinetic variables obtained from the simulations of the zigzag maneuver and turning circles indicate that the ship motion identification matches the target ship

KVLCC2. The RM-SVM predicts the ship trajectory with high accuracy. Thus, the prediction of the 20°/20° zigzag maneuver performed as the training test proves the effectiveness, and the predictions of the 35° and −35° turning circle tests present the generalization ability of the RM-SVM approach. What is noteworthy, the simulations of the 35° and −35° turning circle tests require only several seconds, whereas the full-scale test requires 25 min. Hence, the simulations can present the real-time performance of the RM-SVM, which is crucial for a ship handling simulator. What is more, the accelerations predicted by RM-SVM are highly accurate and can be utilized when taking decisions in ship course and track control.

However, there are some issues which have not been considered in the proposed method. The first is the effect of ship rolls on the ship maneuvering motion, due to the fact that the 3-DOF model was used in this study. The second

issue refers to the fact that the 35° or –35° turning circle tests had just one free running model test result. This implies that the uncertainty analysis of captive and free running model test could not be performed; thus, there is a certain error. The third issue is related with the fact that the scale of ship model used in this paper is 45.7. The scale effects of CFD-SJT and EXP-NMRI were not analyzed in detail, and they can be a source of differences in comparison.

CONCLUSIONS

The RM-SVM based grey box model structure and adaptive tuning for ship motion identification modeling is presented. The key technologies and skills applied are: RM selection, velocity conversion using the similarity rule, and adaptive SVM tuning. The RM-SVM has a simple structure and requires shorter training and simulation times compared with other models. By analyzing earlier studies, we can find that ship modeling based on AI system identification is a time-consuming work, while the RM-SVM simulation requires less time. Illustrative examples presented in the paper demonstrate the generalization ability and feasibility of the RM-SVM approach. Furthermore, this RM-SVM scheme of adaptive tuning used for insensitive band in SVM has been proved to be effective.

In this study, three crucial results were obtained. Firstly, compared with the CFD and other related methods, the prediction accuracy of the proposed RM-SVM method is high. As an identification method for ship maneuvering, the prediction of the RM-SVM makes some progress since the ITTC 2008. Secondly, RM-SVM uses less data and a minor rudder as the identification data than other system identification methods, which yields greater generalization ability. Thirdly, RM shows the approximation ability and provides the base estimation for ship maneuvering.

However, RM-SVM has some inherent drawbacks. It neglects ship hydrodynamic coefficients, such as those in Abkowitz, ship module, or MMG model, and no information about ship flow field is provided, unlike the CFD method. Furthermore, the input variables for SVM are not optimal and need some further theory in the aspect of mechanism principle. For instance, the turbulence of rudder and propeller position cannot be precisely estimated. In this context, future studies should focus on ship maneuvering modeling which will take into consideration sea disturbances, uncertainty analysis, and ship roll.

BIBLIOGRAPHY

1. IMO (International Maritime Organization). Regulatory scoping exercise for the use of maritime autonomous surface ships (MASS), MSC 99-WP.9 Report of the working group, London: IMO, (2018).

2. Knud Benedict, Caspar Krueger, Gerd Milbradt, Michèle Schaub, simulation -augmented maneuvering system to support autonomous ships from the shore in different loading conditions, Autonomous Ship Technology Symposium 2016, Amsterdam, (2016).

3. Guo C. Y., Li X. Y., Wang S., Zhao D. G. A numerical simulation method for resistance prediction of ship in pack ice. Journal of Harbin Engineering University, (2016), 37(2):145-150.

4. ITTC (International Towing Tank Conference). The maneuvering committee, final report and recommendations to the 25th ITTC. Kgs. Lyngby, Denmark: ITTC, (2008).

5. Jia X, Yang Y. Ship motion mathematical model. Dalian, China: Dalian Maritime University Press, (1999).

6. Abkowitz M A. Measurement of hydrodynamic characteristics from ship maneuvering trials by system identification. Transactions of Society of Naval Architects and Marine Engineers, (1980), (88): 283-318.

7. Luo W L, Zou Z J. Identification of response models of ship maneuvering motion using support vector machines. Journal of Ship Mechanics, (2007), 11(6): 832-838.

8. Yin J C, Zou Z J, Xu F. Parametric Identification of Abkowitz Model for Ship Maneuvering Motion by Using Partial Least Squares Regression. Journal of Offshore Mechanics & Arctic Engineering, (2015), 137(3):031301- 031308.

9. Zhang G. Q. Zhang, Zhang X K, Pang H S. Multi-innovation auto-constructed least squares identification for 4 DOF ship maneuvering modelling with full-scale trial data. ISA Transactions, (2015), 58:186.

10. C Källström, Åström, Karl Johan, Identification and Modelling of Ship Dynamics, volume 7015: Lund (Sweden): Identification and Modelling of Ship Dynamics, (1972)

11. Yoon H K, Rhee K P. Identification of hydrodynamic coefficients in ship maneuvering equations of motion by Estimation-Before-Modeling technique. Ocean Engineering, (2003), 30(18):2379-2404.

12. Sutulo S, Soares C. G. Offline system identification of ship maneuvering mathematical models with a global optimization algorithm. Marsim 2015: International Conference on Ship Maneuverability and Maritime

Simulation. Tyne and Wear, United Kingdom: Newcastle University, (2015).

13. Haddara M R, Wang Y. Parametric identification of maneuvering models for ships. International Shipbuilding Progress, (1999), 46(445):5-27.

14. Wang N, Er M J, Han M. Large Tanker Motion Model Identification Using Generalized Ellipsoidal Basis Function-Based Fuzzy Neural Networks Design Automation Conference. Proceedings. ACM/IEEE. IEEE, (1988):205-210.

15. Faller H. D., W. Simulation of Ship Maneuvers Using Recursive Neural Networks [C]. Twenty-Third Symposium on Naval Hydrodynamics, National Academies Press, 2000.

16. Moreira L., Soares C G., Dynamic model of maneuverability using recursive neural networks. Ocean Engineering, (2003), 30(13):1669-1697.

17. Oskin D. D. Neural Network Identification of Marine Ship Dynamics Control Applications in Marine Systems. (2013):191-196.

18. Bai W. W., Ren J. S., Li T. S. Multi-Innovation Gradient Iterative Locally Weighted Learning Identification for A Nonlinear Ship Maneuvering System. China Ocean Engineering, (2018), 32(3):288-300.

19. Zhu M, Hahn A, Wen Y, et al. Identification-based Simplified Model of Large Container Ships Using Support Vector Machines and Artificial Bee Colony Algorithm. Applied Ocean Research, (2017), 68:249-261.

20. Luo W, Li X. Measures to diminish the parameter drift in the modeling of ship maneuvering using system identification. Applied Ocean Research, (2017), 67:9-20.

21. Kijima K, Toshiyuki K, Yasuaki N, et al. On the maneuvering performance of ship with the parameter of loading condition. Jour of The Soc of Naval Architects of Japan, (1990), 168(3): 141-148.

22. Newman J. Marine Hydrodynamics. MIT, 1977.

23. Fossen T I. Handbook of Marine Craft Hydrodynamics and Motion Control. (2011).

24. Ljung L. Perspectives on system identification. Annual Reviews in Control, (2008), 34(1):1-12.

25. Ioannou P A, Sun J. Robust Adaptive Control. Springer London, (2015).

26. Wang X G, Zou Z J, Hou X R, et al. System identification modelling of ship maneuvering motion based on support vector regression. Journal of Hydrodynamics, 2015, 27(4):502-512.

27. IMO, Revision of the interim standards for ship maneuverability ship maneuvering data submitted by the Republic of Korea, (2000), sub-committee on ship design and equipment, 44th session, Agenda item 4.

28. SNAME. Nomenclature for treating the motion of a submerged body through a fluid. Technical and Research Bulletin. New York: The Society of Naval Architects and Marine Engineers, (1950).

29. Norrbin Nils H., Theory and Observations on the Use of a Mathematical Model for Ship Maneuvering in Deep and Confined Waters, Publication No.68 of SSPA. Sweden, (1970)

30. Ho C H, Lin C J. Large-scale linear support vector regression. Journal of Machine Learning Research, (2012), 13(1):3323-3348.

31. Wang X, Zou Z, Ren R, et al. Black-box modeling of ship maneuvering motion in 4degrees of freedom based on support vector machines. Shipbuilding of China, (2014), 55(3):147-155.

32. Sung Y J, Park S H. Prediction of Ship Maneuvering Performance Based on Virtual Captive Model Tests. Journal of the Society of Naval Architects of Korea, (2015), 52(5):407-417.

33. Yasukawa H, Yoshimura Y. Introduction of MMG standard method for ship maneuvering predictions. Journal of Marine Science & Technology, (2015), 20(1):37-52.

34. Liu H, Ma N, Gu X. Maneuvering Prediction of a VLCC Model Based on CFD Simulation for PMM Tests by Using a Circulating Water Channel ASME 2015, International Conference on Ocean, Offshore and Arctic Engineering. (2015):41548-41545.

CONTACT WITH THE AUTHORS

Bin Mei
e-mail: meibindmu@163.com

Licheng Sun
e-mail: 13910219827@163.com

Guoyou Shi
e-mail: allenimitsg@163.com

Dalian Maritime University
NO. 1 Linghai Road
116026 Dalian
China

Xiaodong Liu
e-mail: xdliuros@hotmail.com

Dalian University of Technology
No.2 Linggong Road, Ganjingzi District
Dalian City
Liaoning Province
116024 Dalian
China